NASA/CR—2000-210570

IN/34
2001 018 992

512111

Subcooled Pool Boiling Heat Transfer Mechanisms in Microgravity: Terrier-Improved Orion Sounding Rocket Experiment

Jungho Kim, John Benton, and Robert Kucner
University of Maryland, College Park, Maryland

December 2000

Since its founding, NASA has been dedicated to the advancement of aeronautics and space science. The NASA Scientific and Technical Information (STI) Program Office plays a key part in helping NASA maintain this important role.

The NASA STI Program Office is operated by Langley Research Center, the Lead Center for NASA's scientific and technical information. The NASA STI Program Office provides access to the NASA STI Database, the largest collection of aeronautical and space science STI in the world. The Program Office is also NASA's institutional mechanism for disseminating the results of its research and development activities. These results are published by NASA in the NASA STI Report Series, which includes the following report types:

- TECHNICAL PUBLICATION. Reports of completed research or a major significant phase of research that present the results of NASA programs and include extensive data or theoretical analysis. Includes compilations of significant scientific and technical data and information deemed to be of continuing reference value. NASA's counterpart of peer-reviewed formal professional papers but has less stringent limitations on manuscript length and extent of graphic presentations.

- TECHNICAL MEMORANDUM. Scientific and technical findings that are preliminary or of specialized interest, e.g., quick release reports, working papers, and bibliographies that contain minimal annotation. Does not contain extensive analysis.

- CONTRACTOR REPORT. Scientific and technical findings by NASA-sponsored contractors and grantees.

- CONFERENCE PUBLICATION. Collected papers from scientific and technical conferences, symposia, seminars, or other meetings sponsored or cosponsored by NASA.

- SPECIAL PUBLICATION. Scientific, technical, or historical information from NASA programs, projects, and missions, often concerned with subjects having substantial public interest.

- TECHNICAL TRANSLATION. English-language translations of foreign scientific and technical material pertinent to NASA's mission.

Specialized services that complement the STI Program Office's diverse offerings include creating custom thesauri, building customized data bases, organizing and publishing research results . . . even providing videos.

For more information about the NASA STI Program Office, see the following:

- Access the NASA STI Program Home Page at *http://www.sti.nasa.gov*

- E-mail your question via the Internet to help@sti.nasa.gov

- Fax your question to the NASA Access Help Desk at 301–621–0134

- Telephone the NASA Access Help Desk at 301–621–0390

- Write to:
  NASA Access Help Desk
  NASA Center for AeroSpace Information
  7121 Standard Drive
  Hanover, MD 21076

NASA/CR—2000-210570

Subcooled Pool Boiling Heat Transfer Mechanisms in Microgravity: Terrier-Improved Orion Sounding Rocket Experiment

Jungho Kim, John Benton, and Robert Kucner
University of Maryland, College Park, Maryland

National Aeronautics and
Space Administration

Glenn Research Center

December 2000

Acknowledgments

SUBCOOLED POOL BOILING HEAT TRANSFER MECHANISMS IN MICROGRAVITY: TERRIER-IMPROVED ORION SOUNDING ROCKET EXPERIMENT

Jungho Kim, John Benton, and Robert Kucner
Department of Mechanical Engineering
University of Maryland
College Park, Maryland 20742

SUMMARY

A microscale heater array in conjunction with a video camera was used to provide heat transfer measurements along with video records of the bubbles in earth gravity and microgravity. The heater array was constructed using VLSI techniques, and consisted of 96 serpentine platinum heaters deposited on a quartz substrate. Each heater in the array was 0.27×0.27 mm in size, and had a nominal resistance of 1000 Ω. A new generation of electronic feedback loops was used to keep the temperature of each heater in the array at a specified value, and the variation in the power required to do this was measured. The fluid was FC-72. In order to minimize gas effects, the bulk fluid was degassed by repeatedly pulling a vacuum on the fluid.

The design and construction of a test package for the Terrier-Improved Orion sounding rocket occurred at the University of Maryland between January and September, 1999. This package was then delivered to NASA Wallops and incorporated into the rocket payload and tested. The payload was flown in December, 1999 from Wallops Island, VA. Accelerometers on board the rocket indicated that the rocket provided 200s of high quality microgravity ($<10^{-6}$ g). Heat transfer data from using the electronic feedback loops were obtained. Unfortunately, the VCR malfunctioned, and no video was acquired. To help interpret the sounding rocket data using video images, the test package was redesigned to fly on the KC-135 in April, 2000 when both data and video were obtained.

For all the test cases, the pressure in the chamber was held at atmospheric pressure (T_{sat} = 56 °C) and the bulk temperature was about 20 °C. The wall temperature was stepped down from 85 to 65 °C in 5 °C increments. The gravity level during the series of tests was 10^{-6} g (sounding rocket), 10^{-2} g (KC-135), 1 g (earth gravity), and 1.8 g (KC-135). Data was obtained at 250 Hz from each of the heaters in the array throughout the microgravity period while video data was obtained at 60 Hz.

Preliminary data reduction indicates that there is little effect of gravity on boiling heat transfer at wall superheats below 25 °C, even though there are vast differences in bubble behavior between gravity levels. At all superheats in microgravity, a large primary bubble was observed to move over the surface, occasionally causing nucleation to occur. This primary bubble was surrounded by smaller bubbles which eventually merged with the primary bubble. This primary bubble initially formed by the coalescence of smaller bubbles generated on the surface, but then remained constant in size for a given superheat, indicating a balance between evaporation at the bubble base and condensation on the bubble cap. The size of the primary bubble increased with increasing wall superheat. Most of the heaters under the primary bubble indicated low heat transfer, suggesting that dryout occurred on the heater surface. High heat transfer was associated with the three-phase contact line and the area surrounding the primary bubble where nucleate boiling occurred. Strong Marangoni convection around the bubble was observed to develop in microgravity, forming a "jet" of fluid into the bulk fluid. This "jet" also provided a reaction force on the primary bubble, and kept the bubble on the heater. At a superheat of 30 °C, the microgravity data fell significantly below the 1 and 1.8 g data due to a large part of the heater surface drying out.

INTRODUCTION

An understanding of boiling and critical heat flux in microgravity environments is important to the design of future heat removal equipment for use in space-based applications. Although much research in this area has been performed since the Space Station was proposed, the mechanisms by which heat is removed from surfaces under these environments are still unclear. It is generally felt that heat is removed from a surface by boiling through the

following sequence of events. Before bubble initiation, heat is transferred from the wall to the fluid by natural convection (in gravity environments) and heat conduction through the growing thermal boundary layer. Once a bubble forms, various heat transfer mechanisms are possible (fig. 1): conduction heat transfer and natural convection from the heated wall to the fluid ($Q_{\text{liquid conduction}}$ and $Q_{\text{natural convection}}$), conduction through the vapor layer (Q_{vapor}), conduction and evaporation through the macrolayer ($Q_{\text{macrolayer}}$), evaporation of liquid due to the superheated liquid layer ($Q_{\text{evaporation}}$), and Marangoni (surface tension) convection ($Q_{\text{Marangoni}}$). Of the above mechanisms, it is thought that $Q_{\text{evaporation}}$ and $Q_{\text{microlayer}}$ play dominant roles in the heat transfer process. When the bubble departs from the surface (due to buoyancy forces in gravity or through inertia forces in microgravity), a vortex ring about twice the diameter of the departing bubble is generated, which scavenges away the superheated liquid layer and replaces it with a new layer of cold liquid (Han and Griffith, 1965). The cycle then repeats.

Many of the early experimental studies regarding boiling heat transfer in microgravity environments were first performed under NASA sponsorship in drop towers (See Siegel, 1967 and Clark, 1968 for a review), and were mainly concerned with determining whether or not gravity affected the boiling process. The results of these early experiments were somewhat contradictory, with some experiments showing no effect of gravity on heat transfer and others showing a strong dependence. Much of the discrepancy can be attributed to the relatively short test times that were available since convection effects from before drop initiation could not be eliminated during the short drop time. Visual observations of the boiling process, however, revealed that a large increase in bubble size (up to a few millimeters) occurred under microgravity conditions, with small bubbles coalescing into larger bubbles a small distance from the heater. Siegel and Keshock (1964), for example, found the bubble departure radius to vary approximately as $a^{-1/3}$ for $0.1 < a/g < 1$, and according to $a^{-1/2}$ for lower gravities.

Straub and co-workers have been looking at boiling in microgravity environments under sponsorship of the German Department of Research and Technology since the early 1980s. (Zell, Straub, and Weinzierl, 1984; Vogel and Straub, 1992; and Zell, Straub, and Vogel, 1989, 1990). Investigations were carried out using sounding rockets (test times of up to 6 min) under the TEXUS program, and using NASA's KC-135 aircraft (test times of about 25 s per parabolic flight path). Boiling curves from both wires and flat plates at saturated and subcooled conditions were obtained for Freon 12, Freon 113, and water. Results from their work indicated that gravity has little effect on the overall heat transfer from flat plates-heater temperatures remained constant for given heat fluxes for $\pm 0.03 < a/g < 1.8$, although large increases in the bubble departure radius were observed. Bubble departure was felt to occur as a result of the inertia imparted to the surrounding liquid during bubble growth, which subsequently pulled the bubble away from the heated surface. The researchers concluded that buoyancy effects are replaced by surface tension effects (coalescence and evaporation-condensation) in microgravity, so the overall level of heat transfer remains about the same. It was felt by these authors that the primary heat transfer mechanism was evaporation.

Merte has also performed many experiments over the years. Lee and Merte (1998) describe the results of boiling experiments using R-113 from five space flights between 1992 and 1996. They used a gold film (19×38 mm) sputtered on a quartz substrate as both heater and temperature sensor. Boiling behavior under a wide range of heat fluxes and subcoolings were obtained. They observed eventual dryout of the surface under high heat fluxes at saturated conditions, but steady nucleate boiling at the same heat flux when the subcooling was increased to 22 °C. When steady nucleate boiling was observed, a very large bubble above the surface acted as a reservoir for numerous smaller bubbles growing on the heater surface. The large bubble maintained its size due to a balance between condensation at the top of the bubble and coalescence with the smaller bubbles at its base. Enhancements in the heat transfer of up to 32 percent were observed in microgravity compared to earth gravity. Marangoni convection was also observed to play a significant role in the enhancement of heat transfer since it caused large vapor bubbles to be impelled toward the heater surface and small bubble to migrate to the heater surface. Increased subcooling was associated with an increase in heat transfer level. CHF appeared to decrease significantly in microgravity.

Ohta, et al. (1997) measured the heat transfer, local temperature, and local liquid film thickness during boiling of ethanol on a sapphire substrate using a NASDA TR-1A rocket. The local heat transfer was calculated using a numerical simulation of the transient heat conduction within the central 50 mm of the sapphire substrate. The boundary condition information was provided by a row of platinum, thin film temperature sensors deposited directly onto the surface of the substrate. At high subcooled boiling, small bubbles on the surface of the heater were observed with condensation occurring at the top of the bubbles, and steady state boiling was felt to occur.

Experiments to date have shown that stable, subcooled boiling on flat plates in microgravity environments is possible, although usually with some alteration in heat transfer coefficients. It is important to note, however, that all research pertaining to boiling in microgravity environments has thus far been either of a qualitative nature (photographic studies) with some wall heat flux/wall temperature measurements, analytical work, or numerical

simulations. In the studies where heat transfer coefficients were measured, the heated surfaces were always compa-rable to or much larger than the bubble sizes, so only average heat transfer rates over the entire heated surface were obtained. Very little experimental data is available regarding the local heat transfer rates under and around the bubbles as they grow and depart from the surface. Better understanding of the heat transfer mechanisms involved in the boiling process can be attained by pinpointing when and where in the bubble departure cycle large amounts of heat are removed from the wall, and correlating this information to visual observations of the state of the bubble at those times. Such information can provide much needed data regarding the important heat transfer mechanisms dur-ing the bubble departure cycle, and can serve as benchmarks to validate many of the analytical and numerical mod-els used to simulate boiling. Another technologically important area in which very little research has been performed is the effect of microgravity on critical heat flux. Although it is known that decreasing gravity decreases the critical heat flux level (e.g., Straub, Zell, and Vogel, 1990), very little quantitative data is available. Improved knowledge of the mechanisms controlling the boiling process will improve the reliability and performance of space based heat removal equipment.

In this work, the effects of gravity on highly subcooled pool boiling was studied using an array of micro-scale heaters similar to those used by the author previously for earth gravity measurements (Rule and Kim, 1999) and for microgravity saturated conditions (Kim, Yaddanapuddi, and Mullen, 2000). In this effort, however, a new experimental apparatus was designed and built to fly on the Terrier-Orion sounding rocket. Additional data was taken subsequent to this flight using the same rig, but on the KC-135.

Test Apparatus

Heater array.—Local heat flux measurement and temperature control was performed using an array of platinum resistance heater elements deposited on a quartz wafer in a serpentine pattern. Each of these elements was 0.27×0.27 mm in size, had a nominal resistance of 1000 Ω, and a nominal temperature coefficient of resistance of 0.002 K^{-1}. Ninety-six individual heaters were arranged in a square array about 2.7 mm on a side. The reader is referred to Rule and Kim (1999) for details.

Electronics.—The feedback electronics used in this series of tests were similar to those used in previous tests, and are described in Bae, et al. (1999), but were redesigned so that there were four feedback boards each con-taining 24 circuits and one data acquisition/control card. The temperature of each heater in the array was kept at a constant temperature by feedback circuits similar to those used in constant temperature hot-wire anemometry (fig. 2). The op-amp measured the imbalance in the bridge and output whatever voltage was needed to keep the ratio RH/R1 equal to the resistance ratio on the right side of the bridge.

The heater resistance, and thus the heater temperature, was controlled by varying the resistance of a digital potentiometer from Dallas Semiconductor (DS1267). This chip consists of two 10 $k\Omega$ digital potentiometers, each having 256 wiper positions. The two potentiometers in this chip were connected in series to make a single 20 $k\Omega$ potentiometer with 512 wiper positions. Control of the wiper position was performed through a 3-wire serial inter-face to a personal computer and digital I/O card. For the resistor values indicated, a heater of nominally 1000 Ω resistance could be varied over a 350 Ω range. Since the heaters have a temperature coefficient of resistance of nominally 0.002 K^{-1}, the temperature of the heaters could be varied by ~175 K. Since the digital potentiometer had 512 settings, the temperature of the heaters could be changed in ~0.34 K increments. The output of the circuit was the voltage required to keep the heater at a set temperature. The large 200 $K\Omega$ resistor at the top of the bridge was used to provide a small trickle current through the heater, and resulted in a voltage across the heater of about 100 mV even when the op-amp was not regulating. Because all the heaters in the array were at a set temperature, heat conduction between adjacent heaters could be measured and subtracted from the total power supplied to the heater element, enabling the heat transfer from each individual heater to the fluid to be determined.

The data acquisition system was designed to multiplex the output signals of the individual feedback loops so that any individual circuit could be sampled in any order. To acquire the output signal of a particular circuit, the address of that circuit was output from the computer to the data acquisition card, which then acquired a single sample from that particular circuit. The maximum sampling rate for the data acquisition was 50 kHz. If all 96 cir-cuits were being sampled, then each heater could be sampled at a maximum rate of about 500 Hz.

Payload.—Shown on figure 3 is a schematic of the boiling rig used in this study. This rig is similar to what was used in previous studies, but the dome was made smaller so that it would fit in the sounding rocket. The bellows and the surrounding housing allowed the test section pressure to be controlled. A stirrer was used to break up

stratification within the test chamber, while a temperature controller and a series of Kapton heaters attached to the boiling chamber were used to control the bulk fluid temperature. The test chamber was filled with nominally 3 liters of fluid. The fluid was degassed by periodically pulling a vacuum on it over a three day period. The final dissolved gas concentration in the liquid, determined using the chamber temperature and pressure and the properties of FC-72, was $<1.5\times10^{-3}$ moles/mole.

The experiment payload consisted of the boiling chamber, a 30 Hz CCD video camera (Sony XC-75) with a long range microscope lens (VZM 300), a VCR (TEAC V-80AB-F), and a PC-104 based 233 MHz computer (Real Time Devices CMW686GX233-64). An 80 MB PCMCIA flash disk was used as storage. A drawing of the payload showing the major components is shown in figure 4, and a photograph of the final payload is shown on figure 5. The payload was designed to withstand 50 g loads in all directions, much more than the 10 g load expected during launch of the rocket.

Vibration testing.—The experiment payload was integrated with other components of the rocket at NASA Wallops in September, 2000. These other components consisted of the nose cone, the rate control system (RCS), the accelerometers and roll rate sensors (SAMS-FF), the telemetry module, the despin module, and the parachute can. Vibration testing of the payload began in late September, 2000. This series of tests consisted of mounting the payload on a vibration stand and subjecting it to 10 g sine and 10 g random vibrations in the thrust direction as well as two lateral directions perpendicular to each other. The sine test varied the frequency from 10 to 2000 Hz over about 2 min, essentially subjecting each component in the payload to its resonant frequency. Numerous problems surfaced during the course of the vibration testing. Problems with the experiment payload included transformers and capacitors vibrating loose and falling off, as well as the heater array vibrating out of its socket within the boiling chamber. It was found that while the overall structure was sound, individual components tended to become loose of fall off if not staked down. Once this was realized, the entire experimental payload was disassembled and RTV was used to hold all component in place. Problems with the VCR were also encountered. The vibration testing damaged two separate VCRs, before it was decided to shock mount the VCR. Once this was done, the VCR passed the vibration tests without a problem. The payload finally passed the vibration tests on November 5, 2000. Earth gravity data was obtained on November 22, 1999, to provide a baseline comparison with the microgravity data.

Flight Tests

Sounding rocket.—Launch of the sounding rocket from Wallops Island occurred on December 17, 1999, and 200 sec of very high quality microgravity (10^{-6} g) with a maximum roll rate of 0.2°/s was achieved in all three axes. All vehicle systems worked flawlessly. A maximum altitude of 164 km was reached. Splashdown occurred about 40 miles off the coast, and the payload was spotted by aircraft and picked up by the Coast Guard. A schematic of the flight trajectory provided by SAMS-FF is shown on figure 6. Telemetry during the flight indicated that data acquisition initiated and data at all points in the test matrix were completed. Data was taken with the fluid at 1 atm ($T_{sat} = 56$ °C) and a subcooling of 36 °C at a frequency of 250 Hz/heater. The first point in the matrix was a nucleation run where the heater temperature was set to about 110 °C in order to start nucleation. The wall temperature was then decreased from 85 °C down to 65 °C in 5 °C increments. Data was collected for 25 sec at each temperature. The sequence from 85 °C down to 65 °C was then repeated.

Data from the flash disk was successfully recovered from the payload the next morning. It was found that the VCR had failed to record, however, despite the shock mounting. The cause of this malfunction is currently not known, but is thought to be related to the orientation of the VCR in the payload. VCRs similar to those used in this test were successfully used in previous sounding rocket tests (Dartfire), but were mounted "right side up" relative to the nose of the rocket in these tests. The VCR in our payload was mounted "upside down," and this may have caused the tape to move off the drive momentarily during the launch, then not seat properly. No problems with the VCR were found during post-flight tests.

KC-135.—In order to obtain additional data including video data, the experiment payload was repackaged to fly on the KC-135. Design of this package and the stress analysis were performed between January and March, 2000. A photograph of this test rig is shown on figure 7. The package was flown in late April, 2000, from the NASA Glenn Research Center. The same heater array used in the sounding rocket flight was used during the aircraft tests in order to minimize variation in heat transfer due to different nucleation site distributions. Flying the experiment on the KC-135 allowed data to be obtained at high-g levels as well. Earth gravity data was taken numerous times after the KC-135 flights were completed.

The acceleration environment in the KC-135 was measured using the same SAMS-FF components used to measure acceleration in the sounding rocket. The accelerometers, however, could only measure acceleration to ±1.25g, so the actual g-level during the high-g portion of the parabola can only be estimated to be between 1.6 and 1.8 g.

DATA REDUCTION

The energy supplied to the heater can be calculated from the voltage across the heater and the heater resistance (q_{raw}). Part of this energy is lost through the substrate by conduction (q_{sc}), and part is transferred to the fluid (q). Since the latter quantity is what is desired, q_{raw} must be corrected to account for substrate conduction. The magnitude of this correction was determined as explained below.

The processes associated with boiling on any given heater can be identified from the heat flux variation with time. The term "boiling" in this work refers to the rapid growth and removal of bubbles, either by coalescence or buoyancy (in earth gravity), as indicated by the heat flux traces. The term "liquid" refers to liquid coming into contact with a heater without phase change for a relatively long time-such a situation could occur under natural convection conditions, or on a heater that is not influenced by bubbles nucleating around it. The term "vapor" refers to vapor coming into contact with the heater for a relatively long time-such a situation could occur when a large bubble covers a heater. The heat transfer from the wall to the fluid is very low in this case since the vapor insulates the surface.

Times when vapor covered the surface could be identified by the characteristically low and relatively steady heat flux-an example is shown on figure 8. Heat flux traces and the corresponding video revealed that boiling on any individual heater was interrupted by periods of low heat flux during which vapor covered the heater. Heat transfer to the bulk liquid during this time was minimal since the heaters were effectively insulated from the liquid, and was taken to be a measure of substrate conduction (q_{sc}) and was subtracted from q_{raw} to obtain the heat flux from the wall to the fluid. The uncertainty of in q_{sc} was estimated to be 1 W/cm^2. The distribution of q_{sc} on the surface at a temperature of 85 °C is shown on figure 9. Higher values are observed towards the edge of the array and in the corners, as expected.

RESULTS

Bubble behavior.—At all superheats in microgravity, a large primary bubble was observed to move over the surface, occasionally causing nucleation to occur. This primary bubble moved in a circular path at the higher superheats, and more randomly on the surface at lower superheats. Photographs of the bubble behavior at three superheats during microgravity from the bottom and side are shown on figure 10. This primary bubble was surrounded by smaller satellite bubbles which eventually merged with the primary bubble. The primary bubble initially formed by the coalescence of satellite bubbles generated on the surface, but then remained relatively constant in size for a given superheat, indicating a balance between evaporation at the bubble base and condensation on the bubble cap. The size of the primary bubble increased with increasing wall superheat. Strong Marangoni convection around the bubble was observed to develop in microgravity, forming a "jet" of fluid into the bulk fluid. This "jet" also provided a reaction force on the primary bubble, keeping the bubble on the heater.

In high-g environments, many satellite bubbles were observed on the surface at high superheat, with progressively fewer bubbles at lower superheats. Photographs of boiling from below the heater are shown on figure 11. At the lowest superheat, only natural convection was observed on the surface.

Boiling curve.—Boiling curves were generated from data taken on the sounding rocket, the KC-135, and in earth gravity. The KC-135 data was split into microgravity and high-g data, with boiling curves being generated for each. Comparison of this data with microgravity and earth gravity data taken at saturated conditions using a different heater array and test rig (see Kim, et al., 2000) is shown on figure 12. Significant differences between earth gravity, high-g, and microgravity data are observed. First, all of the subcooled heat fluxes (the data taken during this program) are significantly higher than those for saturated conditions due to the increase in the natural convection heat transfer. Part of the difference in heat fluxes could, however, be due to different nucleation site density distributions since two different heater arrays were used. Second, earth gravity heat fluxes are seen to be lower than both the microgravity and high-g data taken on the KC-135 at superheats below 25 °C. The sounding rocket data falls between the two. It should be noted that the earth gravity data taken before the sounding rocket was launched and after the KC-135 data was taken (almost eight months apart) agree, indicating that both the heater array and control

electronics were stable throughout the test program. Calibration of the heater array before the sounding rocket launch and after the KC-135 tests were completed revealed very little shift in the calibration, further indicating that the electronics and heater array were stable. The differences between the boiling curves are therefore due to some change in the boiling structure on the surface. Third, the microgravity data and high-g data taken in the KC-135 are seen to agree with each other for wall superheats below 25 K, despite the large difference in bubble behavior on the surface. Fourth, the microgravity heat fluxes at the highest wall superheat (30 °C) fall below those for earth gravity and high-g environments due to the primary bubble covering a large portion of the heater in microgravity. This is discussed further in a later section.

The reason for the shift in the boiling curve between the earth gravity data and the other data is not currently known. It is interesting that both the microgravity and high-g data fall above the earth gravity data, indicating that shifts in the boiling curve are not monotonic with gravity. It is planned to take additional data on the KC-135 in late January, 2001, to see if this behavior is reproducible.

Space and time resolved heat transfer.—Space resolved heat transfer distributions on the array at three superheats are shown on figure 13, where each heater has been colorized according to the heat transfer (this heat transfer has been corrected for substrate conduction). Low heat transfer is associated with the dry area underneath the primary bubble, while large amounts of heat transfer occur during satellite bubble growth and departure and on the heaters cooled by natural convection. Occasionally, a satellite bubble grew large enough that the dry area underneath it became larger than a single heater, causing the heat flux from that heater to drop to a low value.

Boiling curves obtained from those areas of the heater on which boiling occurred (i.e., the heaters are ignored when only natural convection occurs on the heater, or if the heater goes dry due to an overlying bubble) are shown on figure 14. It is seen that this "boiling heat flux" is quite independent of the gravity level even at the highest wall superheat, indicating that the small scale bubble heat transfer is independent of the gravity level. This suggests that if one is able to predict the extent of the dry area, then one should be able to predict the microgravity boiling curve from earth gravity boiling heat flux data.

CONCLUSIONS

A payload to study subcooled boiling in microgravity was designed and built. This payload was flown on the Terrier-Orion sounding rocket in December, 1999. 200 sec of high quality microgravity were obtained. Additional data at high-g and in microgravity were obtained on the KC-135 in April, 2000. Earth gravity data were obtained before the sounding rocket flight, as well as before and after the KC-135 flights. Visual data were acquired for all runs except the sounding rocket flight. Boiling curves for the microgravity and high-g heat flux levels were similar, except at the highest wall superheat. The earth gravity heat fluxes were slightly lower than the high-g heat fluxes at all superheats. The space and time resolved heat transfer revealed low heat transfer associated with the large "primary" bubble that forms in microgravity, and large amounts of heat transfer with the satellite bubbles. The heat flux associated with the satellite bubbles were similar to the heat fluxes obtained at earth and microgravity levels, indicating little effect of gravity on the small scale boiling.

REFERENCES

Bae, S., Kim, M.H., and Kim, J.: "Improved Technique to Measure Time and Space Resolved Heat Transfer under Single Bubbles during Saturated Pool Boiling of FC-72," Experimental Heat Transfer, Vol. 12, No. 3, 1999, pp. 265–278.

Clark, J.A., 1968: "Gravic and Agravic Effects in Cryogenic Heat Transfer," Advances in Cryogenic Heat Transfer 87, Vol. 64, pp. 93–102.

Han, C.Y., and Griffith, P., 1965: "The mechanism of heat transfer in nucleate pool boiling—Part II," International Journal of Heat and Mass Transfer, Vol. 8, pp. 905–914.

Kim, J., Yaddanapuddi, N., and Mullen, J.D.: "Heat Transfer Behavior on Small Horizontal Heaters During Saturated Pool Boiling of FC-72 in Microgravity," accepted for publication in Microgravity Science and Application, 2000.

Lee, H.S., and Merte, H., 1998: "Pool boiling phenomena in microgravity," Proceedings of the 11th International Heat Transfer Conference, Kyongju, Korea, Vol. 2, pp. 395–400.

Ohta, H., Kawaji, M., Azuma, H., Kawasaki, K, Tamaoki, H., Ohta, K, Takada, T., Okada, S., Yoda, S., and Nakamura, T., 1997: "TR-1A Rocket Experiment on Nucleate Boiling Heat Transfer Under Microgravity," ASME-MEMS, HTD-Vol. 354, pp. 249–256.

Rule and Kim, J.: "Heat Transfer Behavior on Small Horizontal Heaters During Pool Boiling of FC-72," Journal of Heat Transfer, Vol. 121, No. 2, May, 1999, pp. 386–393.

Siegel, R., 1967: "Effects of Reduced Gravity on Heat Transfer," Advances in Heat Transfer, Vol. 4, Academic Press, New York/London, pp. 143–228.

Siegel, R., and Keshock, E.G., 1964: "Effects of Reduced Gravity on Nucleate Boiling Bubble Dynamics in Saturated Water," Journal A.I.Ch.E. 4, Vol. 10, pp. 509–517.

Straub, J., Zell, M., and Vogel, B., 1990: "Pool Boiling in a Reduced Gravity Field," Proceeding of the 9th Int. Heat Transfer Conference, Jerusalem, Israel, Hemisphere, pp. 91–112.

Vogel, B., and Straub, J., 1992: "Single Bubble Experiments in Pool Boiling," Proceedings of VIII European Symposium on Materials and Fluid Sciences in Microgravity, Brussels, Belgium, ESA SP–333 pp. 879–886.

Zell, M., Straub, J., and Vogel, B., 1989: "Pool Boiling under Microgravity," Journal of PhysicoChemical Hydrodynamics, Vol. 11, No. 5/6, pp. 813–823.

Zell, M., Straub, J., and Vogel, B., 1990: "Heat Transfer in Pool Boiling under Microgravity," Soviet Journal of Low Temperature Physics 16(5), pp. 323–324.

Zell, M., Straub, J., and Weinzierl, A., 1984: "Nucleate Pool Boiling in Subcooled Liquid under Microgravity–Results of Texus Experimental Investigations," Proceedings of the 5th European Symposium on Material Sciences under Microgravity, Schloss Elmau, ESA SP–222, pp. 327–333.
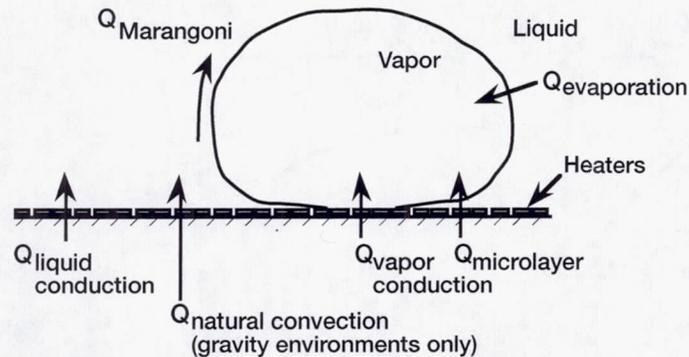
Figure 1.—Various heat flow paths from a heated wall to a bubble growing above a heated surface.
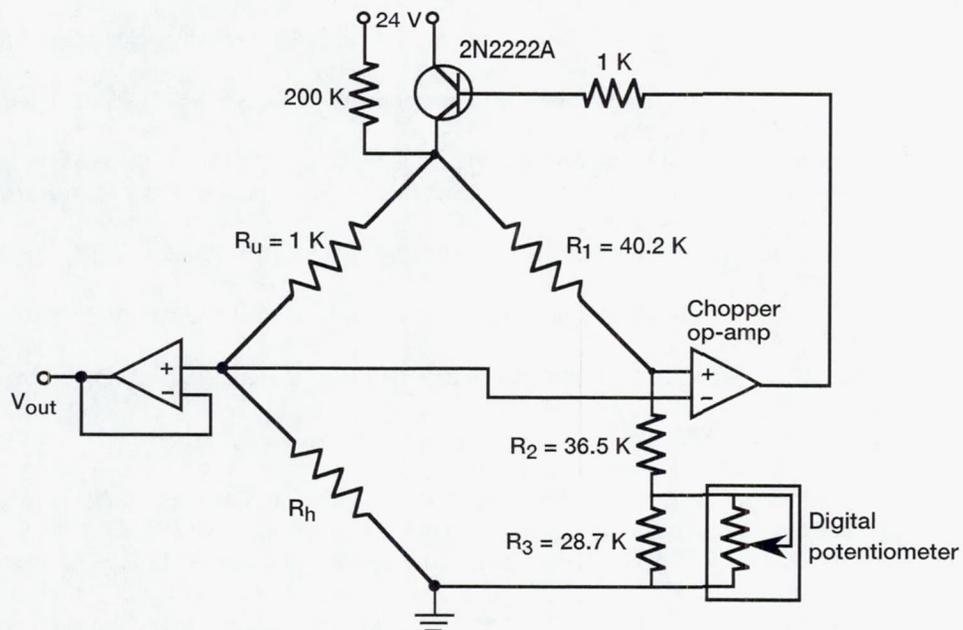
Figure 2.—Schematic of an electronic feedback loop.
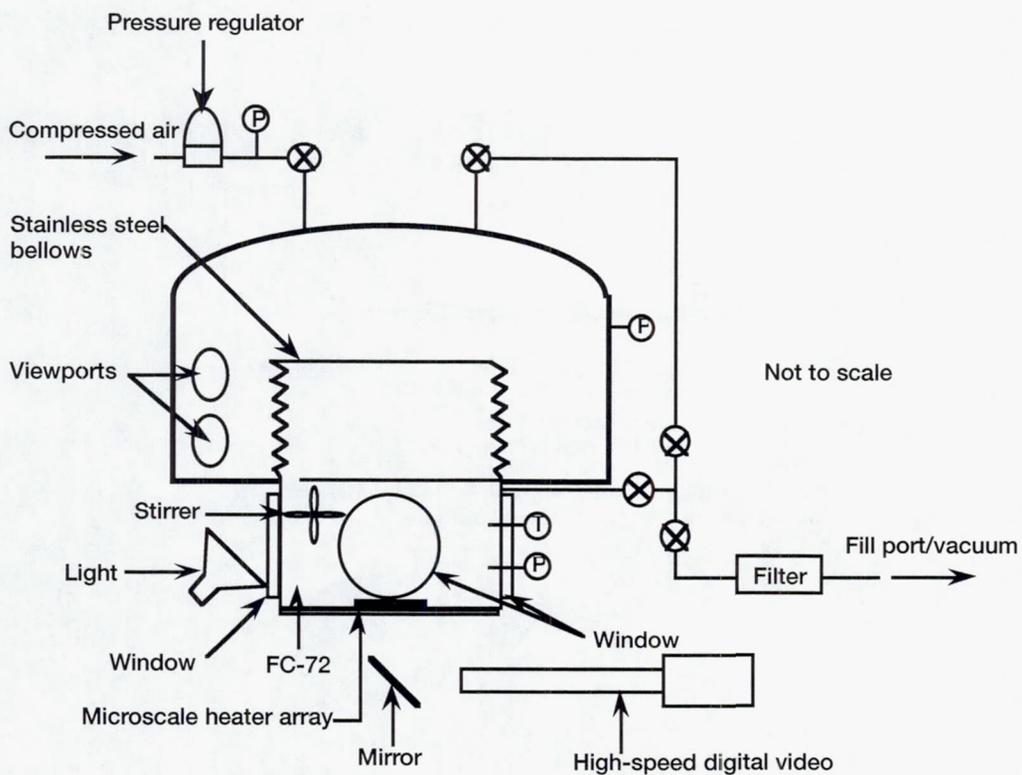

Figure 3.—Schematic of experimental apparatus.
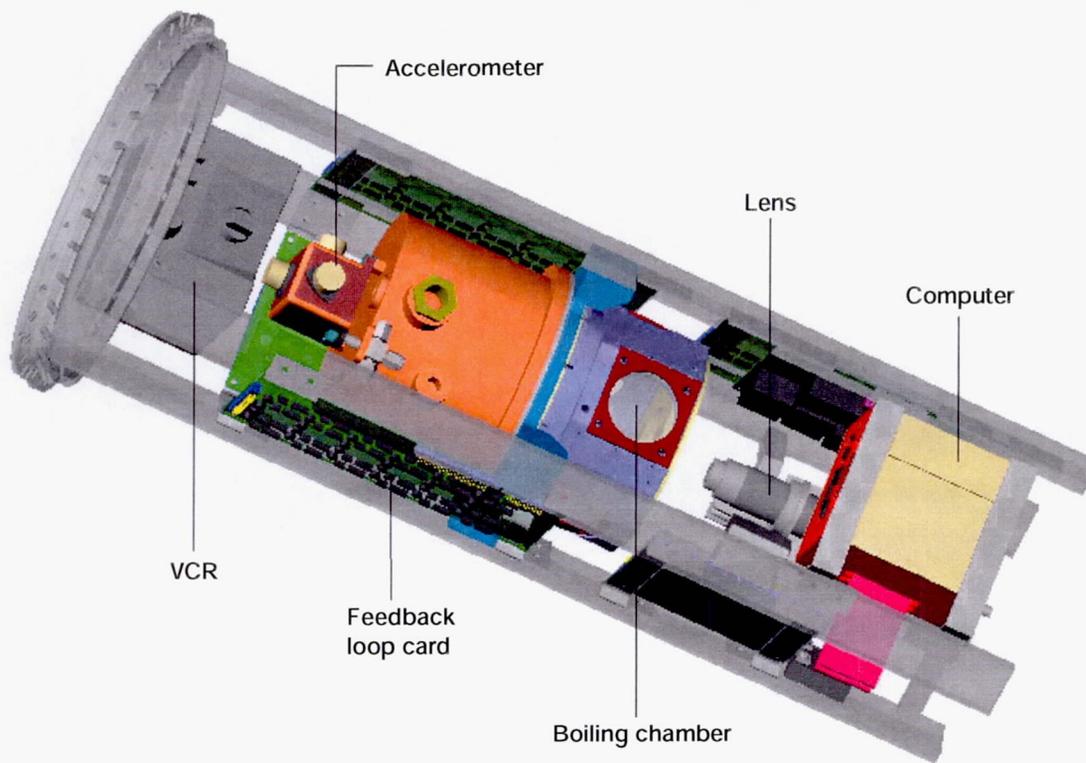
Figure 4.- Solid model of sounding rocket payload.
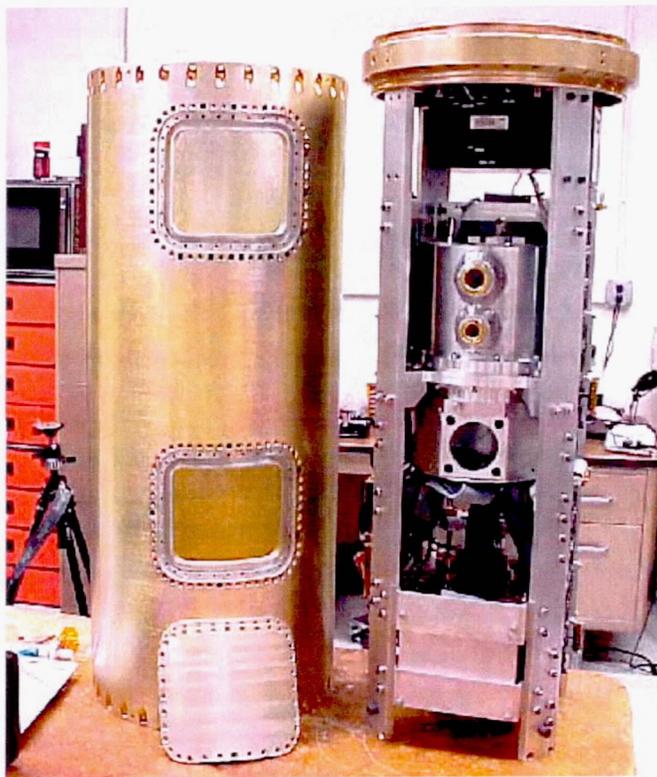
Figure 5.- Photograph of experimental apparatus.
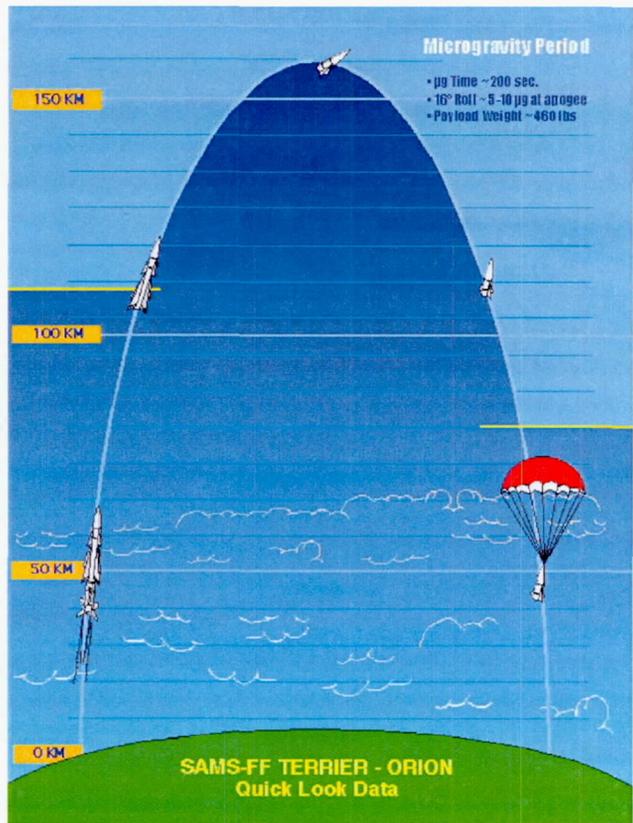
Figure 6.- Sounding rocket flight trajectory.

Figure 7.- Sounding rocket payload on KC-135.
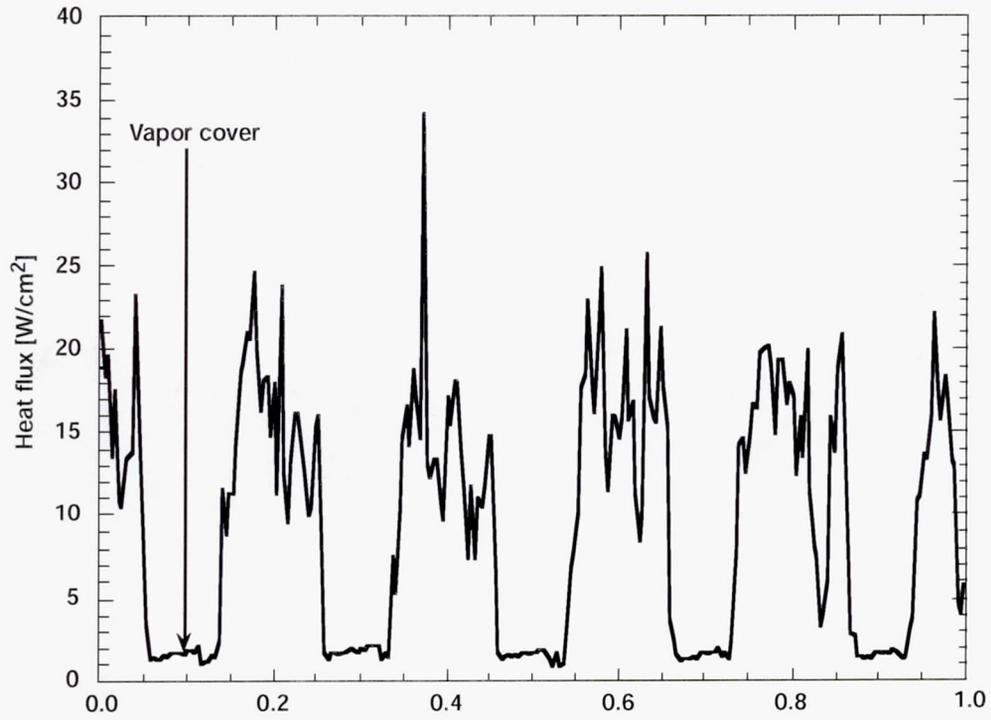
Figure 8.- Heat-flux signal from a single heater in the array (heater #32, wall superheat = 25 °C).
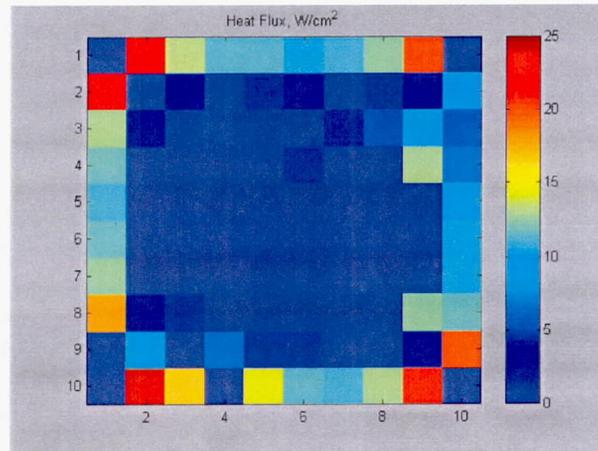
Figure 9.- Substrate conduction distribution on heater surface at 85 °C.
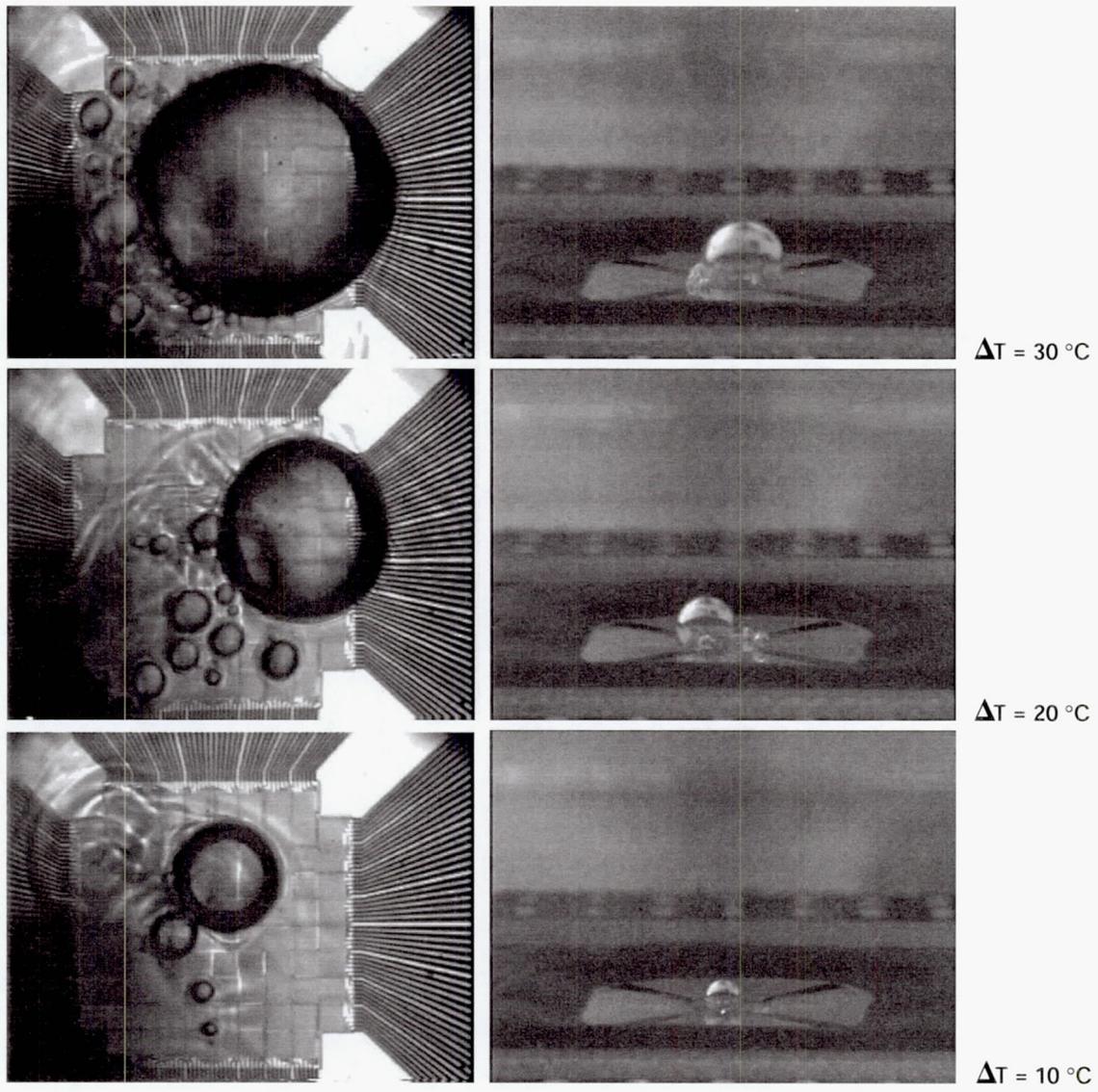
Figure 10.-   Bubble behavior at three superheats during microgravity.

ΔT = 30 °C ΔT = 20 °C ΔT = 10 °C
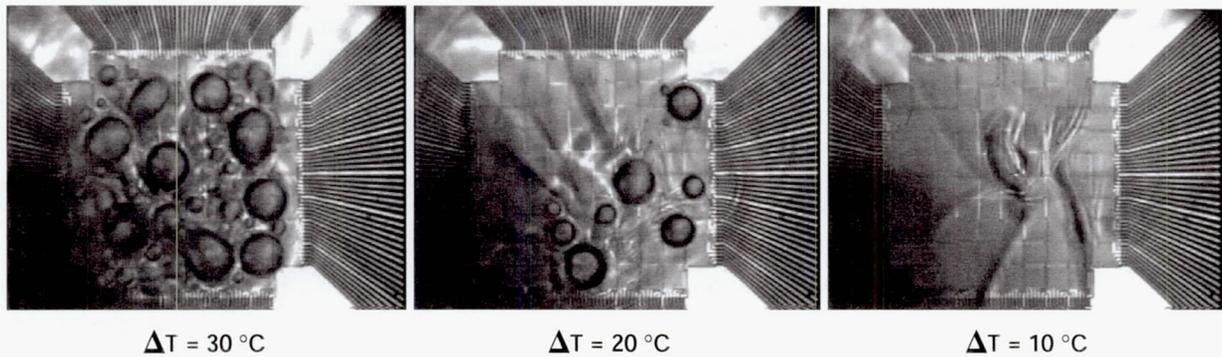
Figure 11.-   Photographs of boiling in the high-g environment.
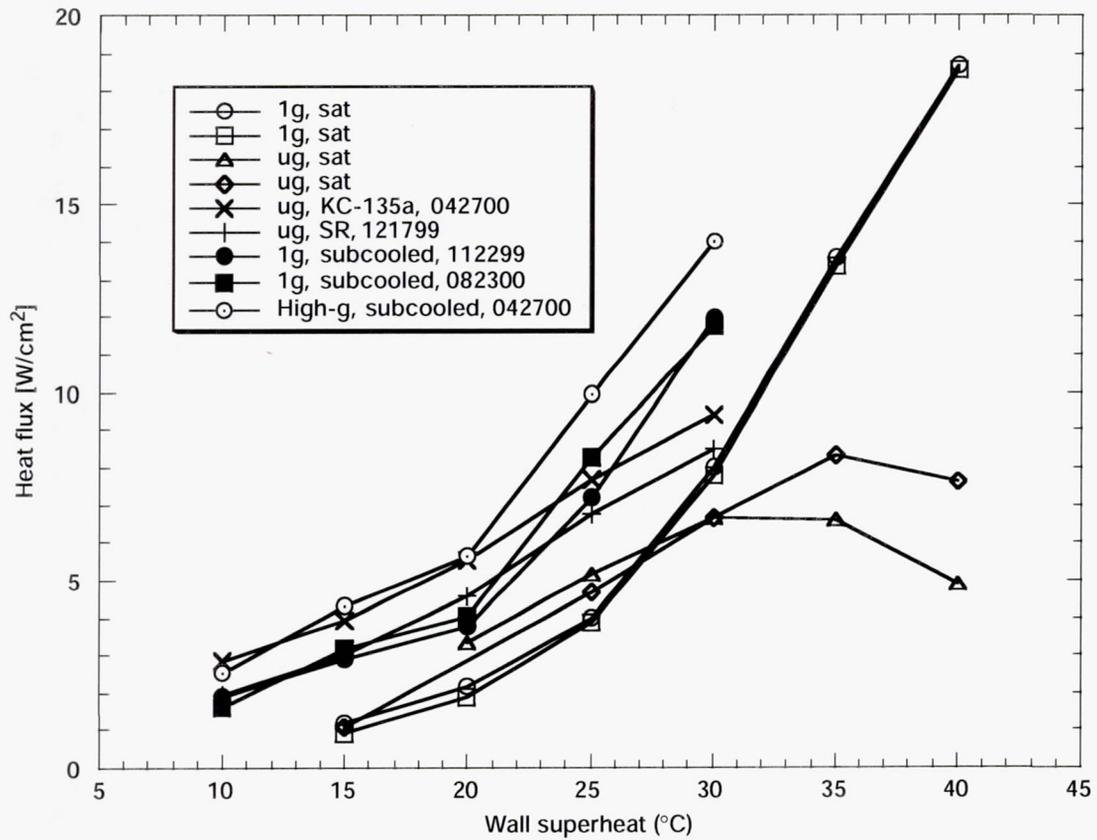
Figure 12.- Boiling curves in earth and microgravity at saturated and subcooled conditions.

Superheat = 30 K   Superheat = 20 K   Superheat = 10 K
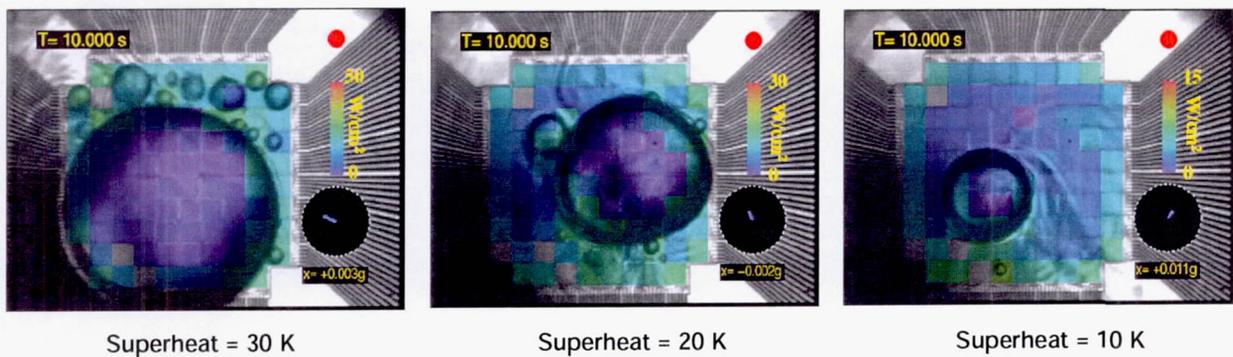
Figure 13.- Spatially resolved heat transfer distributions on the array in microgravity.
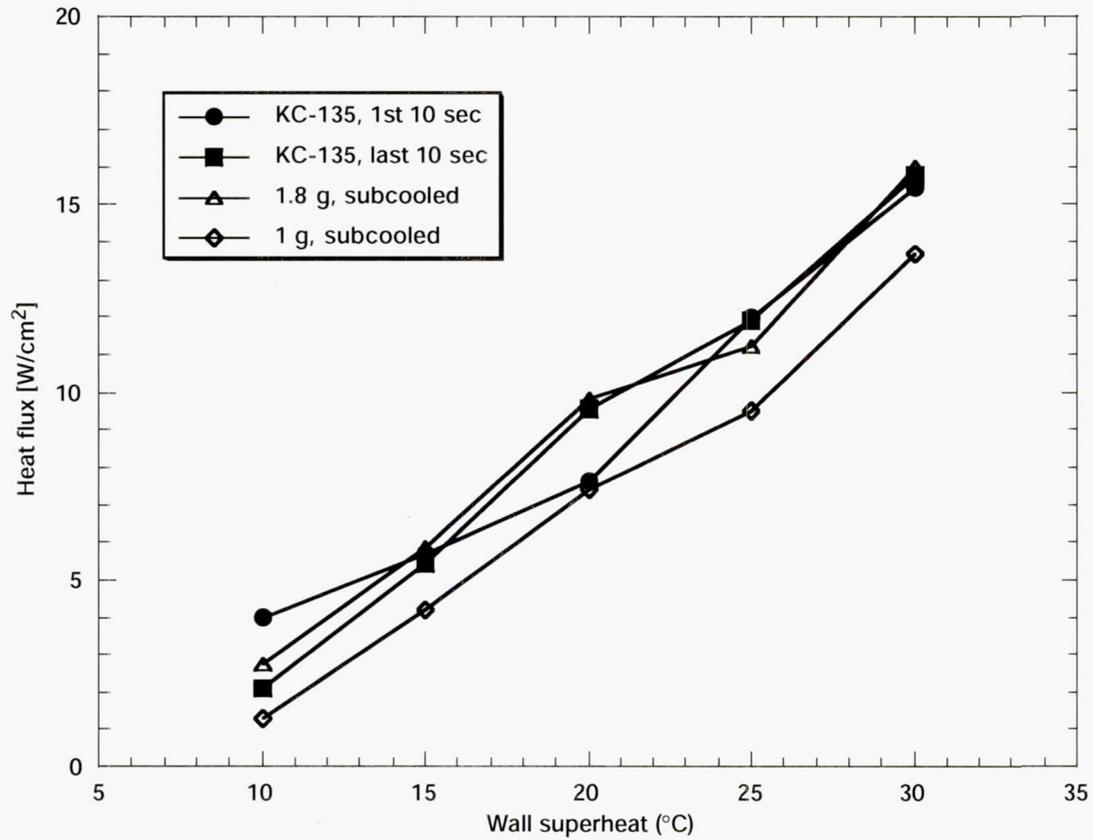
Figure 14.- Boiling heat flux in microgravity, earth gravity, and high-g.

REPORT DOCUMENTATION PAGE

1. AGENCY USE ONLY (Leave blank)	2. REPORT DATE	3. REPORT TYPE AND DATES COVERED
	December 2000	Final Contractor Report

4. TITLE AND SUBTITLE

Subcooled Pool Boiling Heat Transfer Mechanisms in Microgravity:
Terrier-Improved Orion Sounding Rocket Experiment

6. AUTHOR(S)

Jungho Kim, John Benton, and Robert Kucner

5. FUNDING NUMBERS

WU–101–53–00–00
NAG3–2228

7. PERFORMING ORGANIZATION NAME(S) AND ADDRESS(ES)

University of Maryland
Department of Mechanical Engineering
College Park, Maryland 20742

8. PERFORMING ORGANIZATION REPORT NUMBER

E–12536

9. SPONSORING/MONITORING AGENCY NAME(S) AND ADDRESS(ES)

National Aeronautics and Space Administration
Washington, DC 20546–0001

10. SPONSORING/MONITORING AGENCY REPORT NUMBER

NASA CR—2000-210570

11. SUPPLEMENTARY NOTES

Project Manager, John McQuillen, Microgravity Science Division, NASA Glenn Research Center, organization code 6712, 216–433–2876

12a. DISTRIBUTION/AVAILABILITY STATEMENT

Unclassified - Unlimited
Subject Category: 34   Distribution: Nonstandard

Available electronically at http://gltrs.grc.nasa.gov/GLTRS

This publication is available from the NASA Center for AeroSpace Information, 301–621–0390.

12b. DISTRIBUTION CODE

13. ABSTRACT (Maximum 200 words)

A microscale heater array was used to study boiling in earth gravity and microgravity. The heater array consisted of 96 serpentine heaters on a quartz substrate. Each heater was 0.27 mm^2. Electronic feedback loops kept each heater's temperature at a specified value. The University of Maryland constructed an experiment for the Terrier-Improved Orion sounding rocket that was delivered to NASA Wallops and flown. About 200 s of high quality microgravity and heat transfer data were obtained. The VCR malfunctioned, and no video was acquired. Subsequently, the test package was redesigned to fly on the KC-135 to obtain both data and video. The pressure was held at atmospheric pressure and the bulk temperature was about 20 °C. The wall temperature was varied from 85 to 65 °C. Results show that gravity has little effect on boiling heat transfer at wall superheats below 25 °C, despite vast differences in bubble behavior between gravity levels. In microgravity, a large primary bubble was surrounded by smaller bubbles, which eventually merged with the primary bubble. This bubble was formed by smaller bubbles coalescing, but had a constant size for a given superheat, indicating a balance between evaporation at the base and condensation on the cap. Most of the heaters under the bubble indicated low heat transfer, suggesting dryout at those heaters. High heat transfer occurred at the contact line surrounding the primary bubble. Marangoni convection formed a "jet" of fluid into the bulk fluid that forced the bubble onto the heater.

14. SUBJECT TERMS

Boiling; Heat transfer; Nucleate boiling; Microgravity; Sounding rocket; Multiphase flow

15. NUMBER OF PAGES

20

16. PRICE CODE

A03

17. SECURITY CLASSIFICATION OF REPORT	18. SECURITY CLASSIFICATION OF THIS PAGE	19. SECURITY CLASSIFICATION OF ABSTRACT	20. LIMITATION OF ABSTRACT
Unclassified	Unclassified	Unclassified	